

MHONGOOSE commissioning observations of ESO 302-G014 using MeerKAT-64 and 32k mode (Jan 2020)

Erwin de Blok^{1,2,3}

¹ *ASTRON, Netherlands Foundation for Radio Astronomy, Dwingeloo, Netherlands*

² *University of Cape Town, Cape Town, South Africa*

³ *University of Groningen, Netherlands*

version 06-03-2020

Introduction

The observations presented here are a follow-up of the MeerKAT 4k observations of ESO 302-G014 presented in the previous commissioning report. This galaxy was re-observed in January 2020, again with the full MeerKAT array, but this time using the 32k correlator mode, in full polarisation mode. This gave a band width of ~800 MHz and a channel width of 26.1 kHz or 5.5 km/s at 1.4 GHz. The velocity width of the HI emission at 20% of the peak level (as measured from Parkes single-dish observations) is 88 km/s, meaning we expect to detect HI emission in about 16 channels. We expect the data to have a slightly higher signal-to-noise than the previous 4k observations (obtained with a similar observing time) due to the narrower channel widths, which are better matched to the width of the HI spectra.

Standard calibrator J0408-65 was observed as the primary flux and bandpass calibrator, and J0440-43 as the secondary phase calibrator. Target and phase calibrator were observed sequentially, in a cycle of 10 min on target, and 2 min on the secondary calibrator. The primary calibrator was observed twice during the observation, for a total of 20 mins.

Observation details are given below. The total observing times per source listed are prior to any flagging.

<i>Observation ID:</i>	20200106-0015
<i>Observing date/time (UTC):</i>	07-Jan-2020: 15:40—21:53 UTC
<i>Dishes:</i>	59 dishes (m026, m028, m032, m051, m063 not used)
<i>Target and observing time:</i>	ESO 302-G014: 258 minutes
<i>Primary calibrator and observing time:</i>	J0408-65: 20 minutes
<i>Secondary calibrator and observing time:</i>	J0440-43: 50 minutes

The data were transferred to IDIA where we extracted 1000 channels (500 on each side) surrounding the galaxy at 1416.5 MHz, the central frequency of the galaxy. In this observation channel 21456 corresponds to 1416.5 MHz, so channels 20956 to 21956 were extracted. These data were transferred to ASTRON (Netherlands) where they were further reduced with development versions of the MeerKATHI / CARACal pipeline. This pipeline is an effort led by a team from SARAO and RATT and by the Fornax LSP team. More information on the pipeline is available at <https://meerkathi.readthedocs.io/en/latest/> as well as the recent paper by Serra et al. (2019A&A...628A.122S). I am participating in

this effort representing MHONGOOSE. A more extensive description of the pipeline is given in the previous report and is not repeated here.

Data reduction

Initial inspection of the measurement set with `rfigui` showed clean data with only very minor RFI on a few baselines. Though not strictly necessary, we flagged the channels potentially containing Milky Way emission with frequency range 1419.8-1421.3 MHz. To speed up processing we also limited the reduction to 250 channels on either side of the central frequency, so 500 channels in total.

We proceeded to flag the auto-correlations and any data suffering from shadowing. `AOFlagger` (within the pipeline) was then used to flag the calibrator data further based on the Stokes Q and U values. This involved a combination of sigma-clipping, filtering and extending existing flags. In the end all flagging steps described here resulted in ~13% of the cross-correlations in calibrator data being flagged, with most of that due to the flagging of Galactic emission.

We derived the delay, bandpass and gain calibration solutions using the primary and secondary calibrators. All the solutions were well-behaved. Figure 1 shows the bandpass amplitude for 6 dishes. One of the antennas shown there, m021, was reported to show evidence of the 4-channel periodic dips, but this is not apparent in the solutions presented here.

The gain solutions also behaved satisfactorily. The flux of the secondary calibrator B0438-436 (J0440-4333) was found to be 3.55 Jy at a frequency of 1416.5 MHz. The closest measurement in time and frequency in the Australia Telescope Compact Array data base (at 2100 MHz measured in 2011) gives a flux of 3.525 ± 0.016 Jy.

We applied these solutions to the target galaxy data, and split these off twice into two separate measurement sets. The first measurement set retained the original spectral resolution and was later used for the HI imaging. This data set was also flagged with `AOFlagger`. In total (including autocorrelations, Galactic channels, RFI, shadowing), ~30% of the target data were flagged. Only a minor fraction of this was due to RFI.

The second measurement set was produced by averaging by 40 channels in frequency, leading to a measurement set with 12 channels with a channel width of ~1 MHz. This second measurement set was used for self-calibration. We ran three self-cal iterations, with the data subdivided in two equal frequency chunks of ~6.5 MHz. Solutions were derived for each of these chunks with a solution interval of 160 sec. For the three iterations, an increasingly deep automatic clean mask was defined at $(30, 10, 7)\sigma$. Sources in the mask were then cleaned to 0.5σ . Images were created using robust weighting with a robust parameter equal to zero. We imaged a full 2×2 degrees with a pixel size of 2". All chunks were then combined using a common synthesised beam of $7.3'' \times 6.5''$.

The final self-calibrated continuum robust-weighted continuum image has a noise of 17.5 μ Jy. This image is essentially identical to the one presented in the previous report and is not repeated here. To estimate how close to the expected noise the actual noise level is, we created a large area (4×4 degrees), natural-weighted continuum image and measured

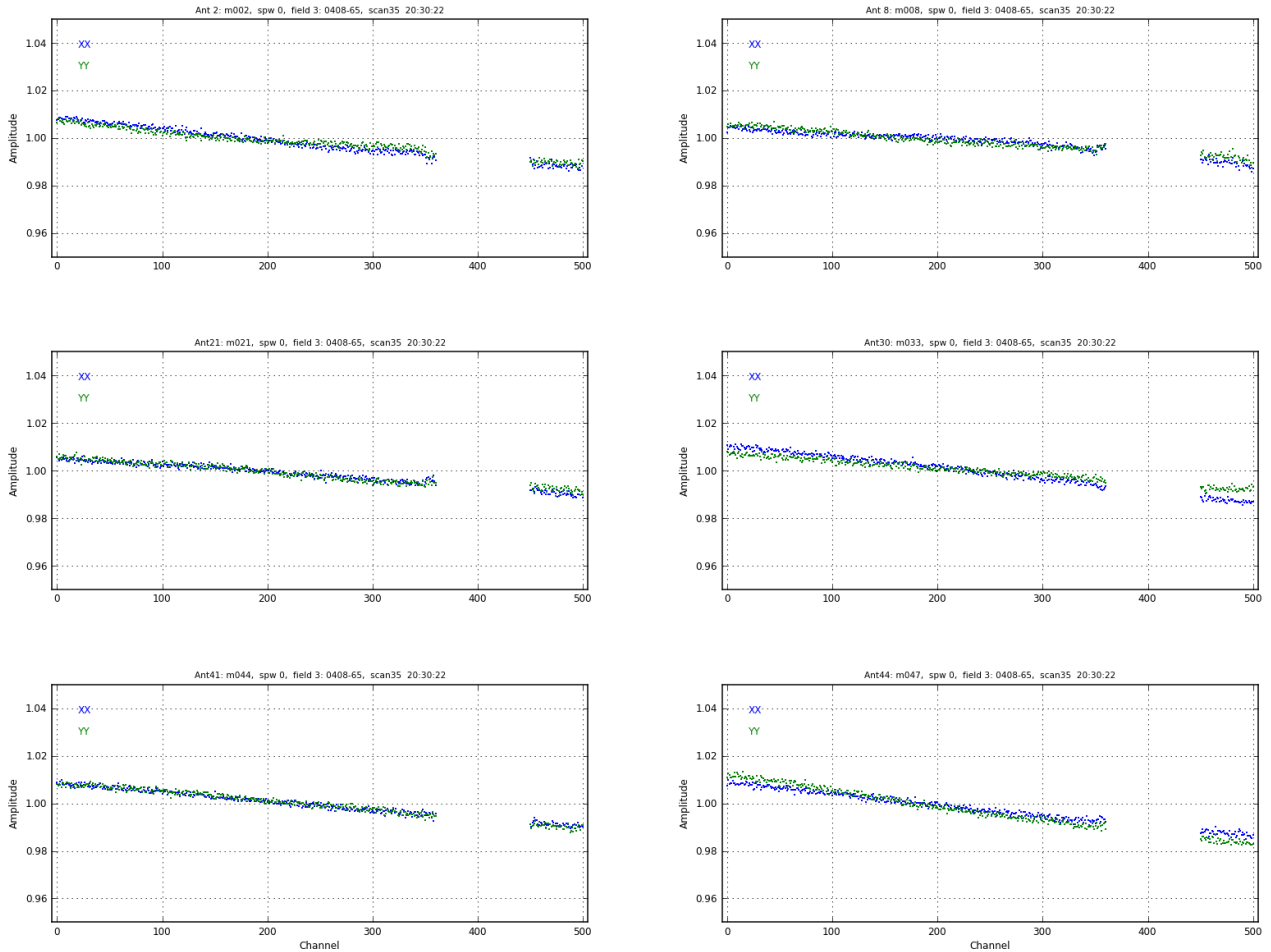


Fig. 1. Examples of bandpass amplitude solutions. Shown are antennas *m002*, *m008*, *m021*, *m033*, *m044*, *m047*. Missing solutions around channel 400 are due to the flagged Milky-Way channels. Solutions of *m021* (one of the antennas reported to suffer from 4-channel periodic dips) behave identically to those of other dishes.

the noise in the far outer field. As even here some sources and low-level residual grating rings are present, we measured the noise at several positions in the outer field and found a value of $14.5 \pm 1.3 \mu\text{Jy}$.

To calculate the expected theoretical noise, we estimate the SEFD of MeerKAT in the 1410-1420 MHz frequency range using Fig. 1 of the "*MeerKAT technical background information - 3 Dec 2018*" document that was issued with the 2018 MeerKAT call for open time proposals¹. We use a value of 377 Jy. With the usual sensitivity equation and the parameters listed in Table 1 we find a theoretical thermal noise of 12.1 μJy . Our measured value is somewhat higher than the predicted value, but consistent with the prediction at just over the 1 sigma level.

In the following we make a comparison with the previously observed 4k data set of the same galaxy. For convenience we list in Table 1 the integration time, bandwidth, number of dishes and noise values of both the 4k and 32k data sets. Note that the sensitivities in this Table refer to the continuum as integrated over the listed bandwidth. These numbers are not indicative of the HI column density sensitivities as these depend on the noise per

¹ Available at <https://goo.gl/XnJ4ZV>

Table 1

data set	integration time (minutes)	number of dishes	bandwidth imaged (continuum)	noise level continuum (measured)	noise level continuum (theoretical) ¹⁾	relative sensitivity (theoretical)
4k	360	61	83.6 MHz	$4.7 \pm 0.8 \mu\text{Jy}$	4.2 μJy	2.88
32k	258	59	13.0 MHz	$14.5 \pm 1.3 \mu\text{Jy}$	12.1 μJy	1

1) This takes into account that ~30% of the data were flagged in both data sets.

individual velocity channel. HI column density sensitivities are discussed in the next section.

For the current 32k data set we find a ratio measured versus theoretical noise of 1.19 ± 0.11 . We can compare this with the values for the 4k data where we find a ratio between measured and theoretical noise of 1.12 ± 0.19 . Most of the difference can be explained by the presence of low-level residual grating rings and faint sources that somewhat inflate the noise values.

Table 1 shows that the ratio of the theoretical noise values of the 32k and 4k data is $\sigma_{32}/\sigma_4 = 2.88$. The observed noise in the natural-weighted 4k data was 4.7 μJy . The ratio of theoretical noise values therefore predicts a noise of 13.5 μJy in the 32k natural-weighted data which is consistent within the uncertainties with the observed value of $14.5 \pm 1.3 \mu\text{Jy}$. Continuum noise values thus behave consistent with the 4k data.

The self-calibration solutions were interpolated and applied to the measurement set with the original spectral resolution. The source list derived from the clean model of the final self-calibrated image was interpolated to the original spectral resolution and used to construct a continuum model that was subtracted in the uv-plane from the target galaxy uv-data. This effectively removed all but the faintest continuum. An additional continuum subtraction step was then done by fitting the first and last 200 channels of the 500 channel data with a linear function and subtracting the fit, resulting in a 300 channel data set containing only the HI emission.

HI data reduction

We created image data cubes of 300 channels straddling the HI emission. These channels were deconvolved using `WSClean` in a two-step process. First a shallow (10σ) clean mask was created automatically which was used to produce a preliminary deconvolved data cube. The source-finding program `SoFiA` was used on that cube to produce an improved clean mask which was applied in a second deconvolution to produce the final data cube. In principle, this could be repeated multiple times to further refine the mask. However, in this case using two iterations was found to be sufficient.

We produced a number of data cubes this way, using various values of the robustness parameter to explore the image quality and the HI morphology at various resolutions. The `robust=1.0` (close to natural-weighted) data set has a noise per channel of 255 μJy (as measured in a continuum-subtracted channel without HI emission). Using the same assumptions as above, we calculate an expected thermal noise of 226 μJy per 26.1 kHz channel, showing that the noise levels in the data are close to the expected noise.

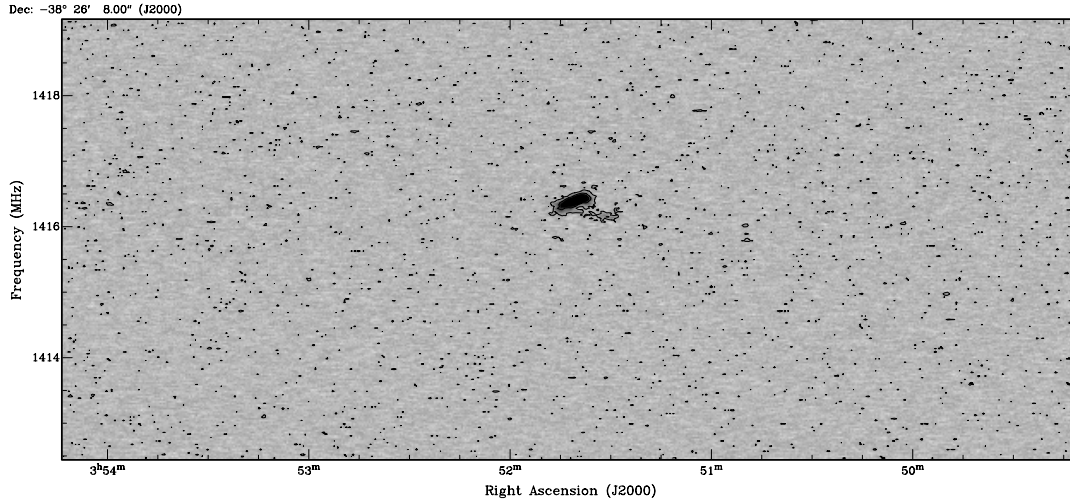


Fig. 2. Position velocity diagram along the RA axis crossing the target galaxy.

Table 2 lists the measured noise value for two values of the robust parameter, along with the corresponding beam size and the HI column density limit. The latter is calculated as a 1σ limit for a single 26.2 kHz channel.

Figure 2 shows a `robust=1.0` position-velocity slice along the RA axis crossing the target galaxy. Note the flatness of the background, the homogeneous distribution of noise peaks and the lack of continuum subtraction features, indicating good quality data. For each robust value, we produced an integrated HI intensity map (zeroth-moment map) by using a simple 3σ clip over the velocity range where HI is observed.

Figure 3 shows the zeroth moment maps and compares them with the previous 4k moment maps. The `robust=0.0` data show intricate details in the HI disk, while the `robust=1.0` map show the presence of low-column density HI around the inner disk. These moment maps will be improved in subsequent analysis using more sophisticated construction methods. The larger number of $>3\sigma$ noise peaks in the 32k moment maps is expected. Both 4k and 32k moment maps were constructed using a 3σ clip. For Gaussian noise, the number of noise pixels $>3\sigma$ in the moment map is proportional to the total number of pixels used as input for that moment map. For the 4k data 3 channels were used as input, for the 32k data 22 channels. For Gaussian noise we thus expect 7.3 times more noise pixels to enter the 32k moment map than the 4k map. The actual ratio (excluding the galaxy) in the `robust=0.0` map is 7.4, showing that the number of noise pixels in the moment map is as predicted and consistent with Gaussian noise.

The 32k data reveal additional details not seen in the 4k data despite the somewhat shorter integration time of the former. This increased column density sensitivity is due to the very different channel widths of the 32k and 4k data. Column densities limits are calculated from (a multiple of) the noise in a channel times the width of that channel (units of $[\text{Jy}/\text{beam}] \cdot [\text{km}/\text{s}]$). In its simplest form, if we have a noise per channel σ_{32} in a 32k channel with width Δv_{32} , then the column density limit is proportional to $\sigma_{32} \Delta v_{32}$. In an identical 4k observation with channels that are 8 times wider, this noise limit will be $\sqrt{8}$ better: $\sigma_4 = (\sigma_{32}/\sqrt{8})$. However, as the channel width is a factor 8 larger, the column density limit in that 4k channel will be $\sigma_4 \Delta v_4 = (\sigma_{32}/\sqrt{8}) \cdot \Delta v_{32} \cdot 8 = \sigma_{32} \cdot \Delta v_{32} \sqrt{8}$. This is a factor 2.8, or 0.45 dex, which explains most of the difference we are seeing in the sensitivities in the moment maps. (The difference in integration time accounts for $\sim 20\%$ only).

Table 2

robust value	noise (μJy)	beam (arcsec)	log N_{HI} (cm^{-2})
0.0	358	8.4 x 7.0	19.57
1.0	255	27.1 x 19.4	18.47

A second contributing effect, alluded to already, is the better match between typical HI line widths and the 32k channel width, compared to the 4k channel width. This avoids that the signal of any HI profile (typically $\sim 10\text{-}15$ km/s wide) is diluted by the "empty" part of the 45 km/s wide 4k channel. This allows for a better discrimination between signal and noise, which in combination with the smaller channel width allows for a lower limit.

Summary

The new 32k HI data show no major issues. The narrower channel width results in an improved column density sensitivity, and, especially for the highest-resolution data, results in an improvement in spatial details compared with the 4k data.

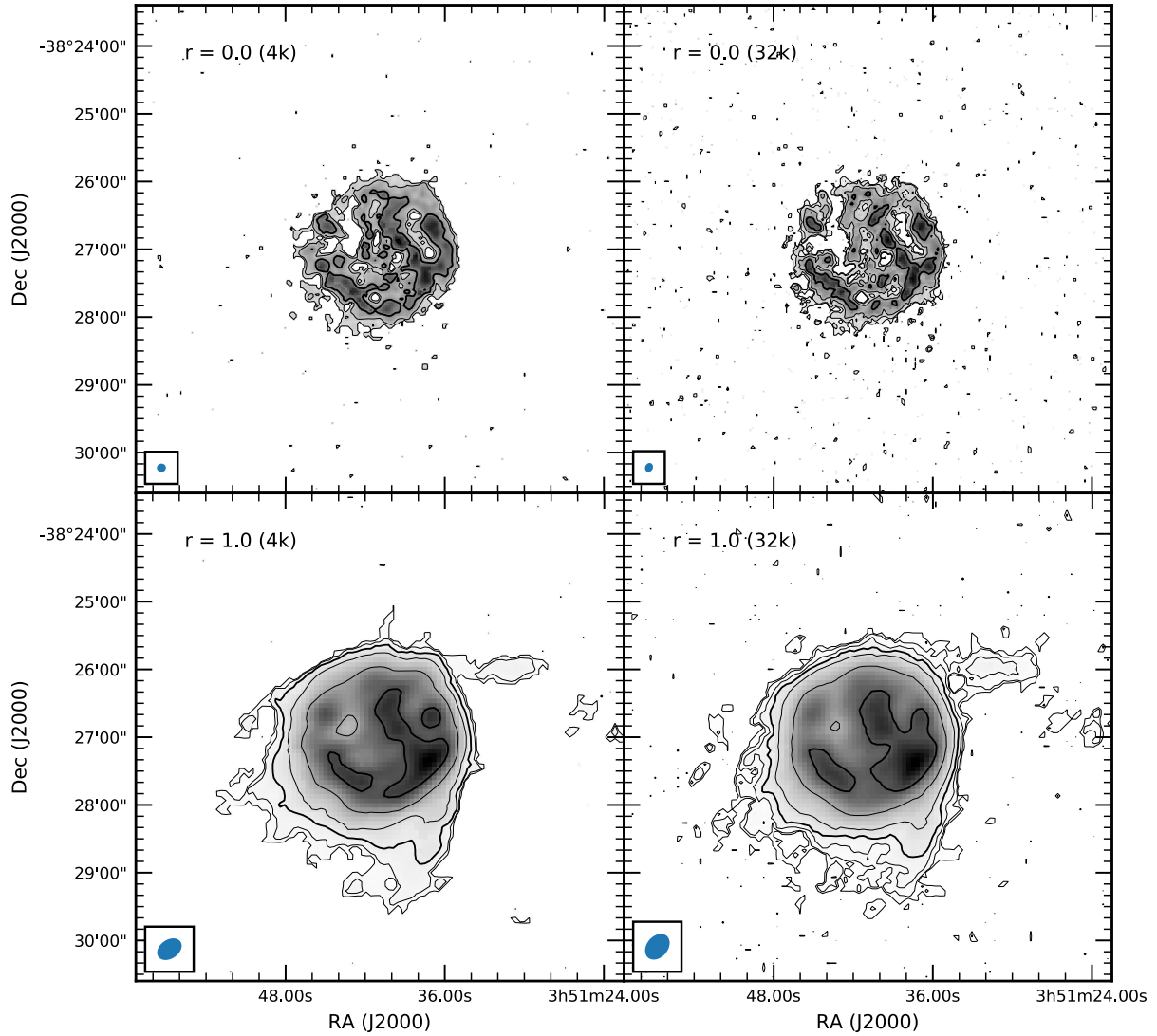


Fig. 3. Integrated HI maps of galaxy ESO 302-G014 for $robust=0.0$ (top row) and $robust=1.0$ (bottom row). Left panels shows the 4k data, right panels the 32k data. The lowest contour in each panel is the 3σ contour. The contour levels for each panel are as follows. Top-left: $(2.9, 5.0, 10.0) \cdot 10^{20} \text{ cm}^{-2}$. Top-right: $(1.2, 2, 5.0, 10.0) \cdot 10^{20} \text{ cm}^{-2}$. Bottom-left: $(0.3, 0.5, 1.0, 2.0, 5.0, 10.0) \cdot 10^{20} \text{ cm}^{-2}$. Bottom-right: $(0.1, 0.2, 0.5, 1.0, 2.0, 5.0, 10.0) \cdot 10^{20} \text{ cm}^{-2}$. In the top panels the $1 \cdot 10^{21} \text{ cm}^{-2}$ level is shown as a thick contour. In the bottom panels both the $1 \cdot 10^{20} \text{ cm}^{-2}$ and the $1 \cdot 10^{21} \text{ cm}^{-2}$ levels are shown as thick contours. The beams are indicated in the lower-left corners. Note that in each case the 32k data reach lower column densities and show more detail than their 4k counterparts. This is due to the channel widths being a better match to the HI line widths than the wide 4k channels. See text for more detailed information.